Plasma Chemistry and Plasma Processing, Vol. 25, No. 1, February 2005 (© 2005)

Microhollow Cathode Discharge Reactor Chemistry

David D. Hsu[1] and David B. Graves[1,2]

Received August 8, 2003; revised May 3, 2004

We discuss the microhollow cathode discharge (MHCD) as a microreactor for endothermic reactions. The high-peak neutral temperature, power density, and ion density of MHCDs may provide a highly reactive environment for these chemistries. Decomposition of ammonia and carbon dioxide are examined. Conversion is found to vary strongly based mainly on residence time. The results are fit to a plug-flow reactor model, and an effective reaction temperature is calculated. The effective reaction temperature in both cases exceeds 2000 K and suggests that thermal processes play an important role in decomposition.

KEY WORDS: Microhollow cathode; microplasma; microreactor; decomposition.

1. INTRODUCTION

Microhollow cathode discharges (MHCDs), because of their small size and high-pressure stability, could be used as a microreactor to process gases. Such microreactors have appeared on so-called 'lab-on-a-chip' configurations, where entire analytical chemical processes, such as DNA PCR, can be miniaturized onto devices smaller than the size of a human hand.(1) This line of thought can be extended to entire chemical processes where a 'system-on-a-chip' could produce small amounts of a chemical point-of-use and on-demand.(2) As the '-on-a-chip' and other microelectromechanical systems (MEMS) technologies mature, microreactors will become more prominent.

The MHCD properties imply that the discharge could be well-suited as a microreactor, particularly for certain classes of reactions. The discharge has a high-power density. These plasmas typically operate at 1–5 W per hole. Simply dividing the power deposited by the hole volume yields a high-power density on the order of several kw/cm^3. By comparison, the analogous calculation on an inductively coupled plasma (ICP) yields a

[1]Department of Chemical Engineering, University of California at Berkeley, Berkeley, CA 94720.
[2]To whom correspondence should be addressed. E-mail: graves@uclink4.berkeley.edu

0272-4324/05/0200-0001/0

power density on the order of 0.1 W/cm^3. One would expect that high-power densities would result in high-peak neutral temperatures in the MHCD. As shown by optical emission thermometry measurements of the plasma, the peak neutral temperature is of the order of 1000–2000 K.[3,4] The high-power density and peak neutral temperature would be ideal for endothermic ($\Delta H_{rxn} > 0$) reactions. High temperatures also would promote the kinetics of a reaction by increasing the Arrhenius rate coefficients. The high gas temperatures are likely the result of the direct current (DC) nature of the discharge in which ion and electron current through the gas (especially in the cathode fall) efficiently transfers energy to the neutral gas. Higher gas pressures available to MHC operation increase equilibrium conversion for mole-decreasing reactions. In addition, reactions could be enhanced by reactive plasma species. Plasma densities have been measured as high as $10^{15}\,\mathrm{cm}^{-3}$.[4]

Few other, if any, high-pressure plasmas can achieve such high temperatures on such a small scale. In dielectric barrier discharge and coronas, neutral gas temperatures are relatively low, thus chemistry is generally thought to be a result of electron-impact processes. As the characteristic dimension of the plasma is on the order of 10^{-4} m, temperature gradients are likely to be on the order of 10^7 K/m. In a typical ICP, characteristic dimensions are usually at least two orders of magnitude higher, resulting in smaller peak gradients of 10^5 K/m. Gradients in other plasma quantities are also likely to be large in MHC's, suggesting that relatively small changes in device design could have significant effects on plasma performance. The key characteristics of the MHC plasma from the point of view of chemical reactions are their very compact size coupled with their extraordinarily high intensity. There are few alternative configurations that couple the size and intensity of the MHC. Thin-film resistive heaters used in MEMS achieve temperatures greater than 1000 K, but suffer from material degradation.[5]

Endothermic reactions were chosen to study the effectiveness of the MHCD as a microreactor. The chemistries and enthalpies are listed in Table 1. The destruction of ammonia into nitrogen and hydrogen (the reverse of the well-known Haber process) could be used as a source of hydrogen. The cracking of carbon dioxide could be used as part of a

Table I. Chemistries Studied and Relevant Thermodynamic Data

Chemistry	Enthalpy (KJ/mol)
$NH_3 \rightarrow \frac{1}{2}N_2 + \frac{3}{2}H_2$	$\Delta H^0 = 46$
$CO_2 \rightarrow CO + \frac{1}{2}O_2$	$\Delta H^0 = 283$

method to dispose of radioactive carbon dioxide resulting from nuclear fuel production[6] or for the production of oxygen.

2. EXPERIMENTAL

The MHC used in this work is based on the early studies of Schoenbach *et al.*[7,8] The MHC is constructed from two molybdenum electrodes sandwiching a mica dielectric (Fig. 1). Molybdenum is used as an electrode because of its low work function and high sputtering threshold.[9] The molybdenum electrodes are 100 μm thick. The dielectric is 260 μm thick. The three layers are epoxied together, and a hole 200 μm in diameter is mechanically drilled through all three layers.

The cathode is supplied with a negative DC voltage through a 100 kΩ ballast resistor. The anode is grounded through a 100 Ω resistor. The plasma current is determined by measuring the voltage drop across the 100 Ω resistor. The plasma voltage is found by measuring the voltage at the MHC with respect to ground.

The apparatus used for microreactor studies is shown in Fig. 2. The gas flow is controlled by a mass flow controller. The gas flows through the microhollow cathode discharge. The bulk of the gas flow exits to a mechanical pump, bypassing any analytical tools. A metering valve upstream of the mechanical pump is adjusted to control the pressure for a given flowrate. Most of the tubing used is 6.4 mm diameter stainless steel tubing so as to minimize the volume of the system. Two capacitance manometer pressure gauges monitor pressure upstream and downstream of the MHC. The MHC is clamped in place by a fiberglass holder. Two concentric o-rings on each side of the MHC minimize leakage. The cathode is oriented downstream of the anode. Some of the gas bleeds through leak valves to an Inficon Transpector 2 mass spectrometer or a

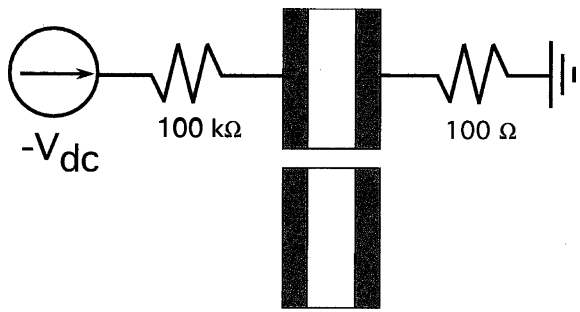

Fig. 1. Microhollow cathode and electrical circuit.

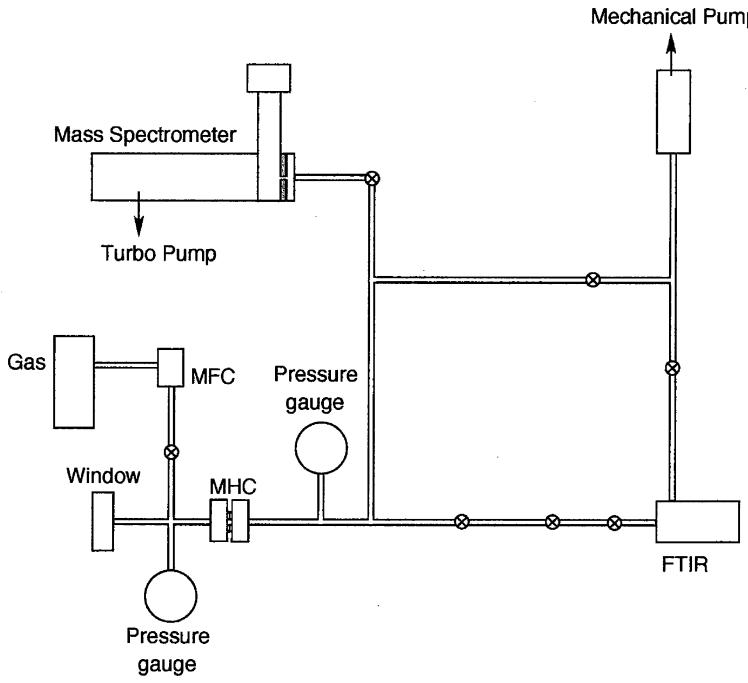

Fig. 2. Apparatus for microreactor studies allowing for simultaneous mass spectrometer and Fourier transform infrared (FTIR) measurements.

MKS On-Line 2010 Fourier transform infrared (FTIR) spectrometer. The mass spectrometer, pumped by a turbo pump, operates at pressures of 1×10^{-6}–1×10^{-5} Torr. The FTIR, with a sampling volume of 1600 cm^3 operates at a few Torr. Operating the FTIR at low pressure allows for concentrations in the sampling volume to reach steady state more quickly than if it were operating at high pressures of the MHC. IR is absorbed by some absolute number of molecules in the gas cell. The MKS software calculates the density based on the spectra. The pressure in the FTIR gas cell is a few Torr, lower than the hundreds of Torr near the MHCD. The measured density will be based then only on a representative fraction of the molecules exiting the MHC, and it is assumed that the flow never is molecular flow as the mean free path is much smaller than tube and valve dimensions. A lumped conductance model, described in Section 4, of the experimental system is developed to verify that the FTIR readings reflect the concentrations in the system and that the resulting percent conversions are accurate. The model is also used to explain surges and dips in the mass spectrometer and FTIR readings.

Two MHCs are also used to test conversion in a series of reactors (Fig. 3). The second plasma may increase the conversion as reactive species may be carried over to the second plasma. The second plasma would also operate at a lower pressure, and thus operate more stably at a given power. Both MHC's are put in the holder shown in Fig. 2. An o-ring 2.5 mm in thickness is placed between the two MHC's. Each MHC has an electrical circuit independent of the other one, but both have power supplies delivering negative voltage through a 100 kΩ ballast resistor. The two grounded anodes face each other in the center of the series system in order to avoid plasma formation between the two MHC's.

3. RESULTS

3.1. Ammonia

The results of cracking ammonia are charted in both the mass spectrometer and the FTIR. Figure 4 shows the mass spectrometer results of one run. The plasma is turned on and off repeatedly to demonstrate the conversion of ammonia. The hydrogen and nitrogen signals in the mass spectrometer increase when the plasma is on. The ammonia signals in the FTIR show a similar response, but hydrogen and nitrogen are not seen in the FTIR because the FTIR cannot detect homonuclear diatomic molecules. By taking the steady-state levels of ammonia when the plasma is on and when the plasma is off, a percent conversion can be calculated. The percent conversion calculated for the FTIR signal is consistent with the value calculated for the mass spectrometer signal. The nitrogen, hydrogen and ammonia signals in the mass spectrometer cannot be compared quantitatively to each other because of different mass spectrometer sensitivities to different molecules. Thus, one cannot assume from Fig. 4 that 10 times more hydrogen is produced compared with nitrogen. The ratios of the different gases in the mass spectrometer also vary from run to run

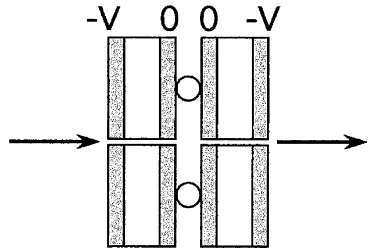

Fig. 3. Microhollow cathode's in series.

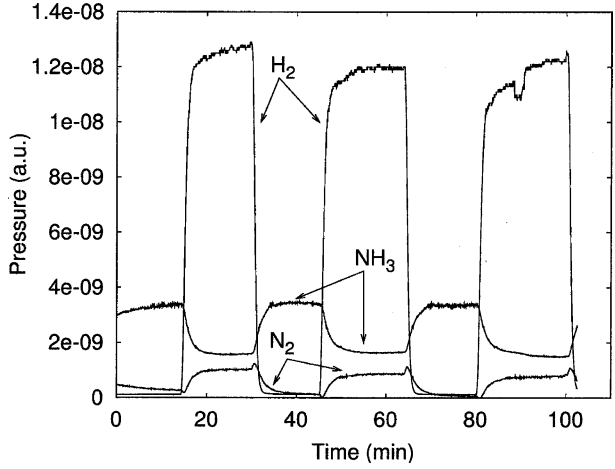

Fig. 4. Mass spectrometer results of ammonia decomposition in an microhollow cathode. Ammonia flow is at 1.5 sccm, with an upstream pressure of 100 Torr. The voltage of the plasma is 480 V and the current is 9 mA.

so a quantitative analysis of the amount of hydrogen and nitrogen produced was not possible.

Conversions for ammonia for different flowrates are shown in Fig. 5. As the flowrate increases, the conversion drops. The conversion data can

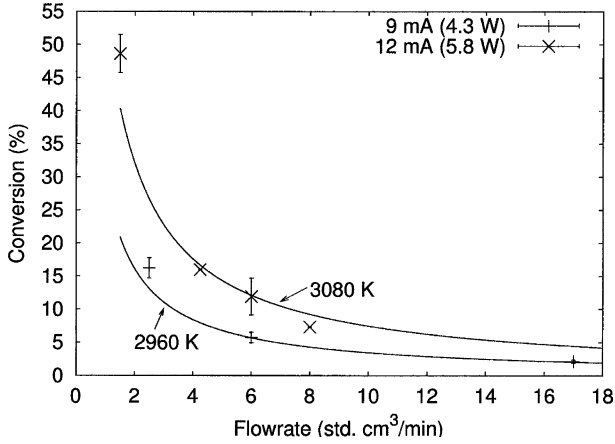

Fig. 5. NH_3 conversion as a function of flowrate for two microhollow cathode powers. Upstream pressure is 100 Torr.

be fit to a plug flow reactor model and kinetic data from the literature.[10,11] Davidson *et al.*[10] provide a pyrolysis mechanism with 21 elementary steps. Konnov and DeRuyck[11] list 50 elementary steps. In order to obtain a first-order rate equation of the Arrhenius form

$$-\frac{\mathrm{d}[\mathrm{NH_3}]}{\mathrm{d}t} = k_0 \exp\left(-\frac{E}{RT}\right)[\mathrm{NH_3}], \tag{1}$$

ammonia conversions are calculated for both models for temperatures from 2000 to 3000 K and for reaction times of 10^{-4} and 10^{-5} s using Kineticus reaction simulation software. The temperature range is chosen to be near the temperature range tested experimentally in the Davidson paper. Although for an ordinary first-order equation, the rate expression should not change with different residence times, the expressions for both literature mechanisms change slightly. The resulting activation energies, E, and pre-exponential factors, k_0, from the two different rate mechanisms and two different residence times are averaged to obtain the following rate expression:

$$-\frac{\mathrm{d}[\mathrm{NH_3}]}{\mathrm{d}t} = 4.23 \times 10^{13}\mathrm{s}^{-1} \exp\left(\frac{-5.19 \times 10^5 \mathrm{J\,mol}^{-1}}{RT}\right)[\mathrm{NH_3}] \tag{2}$$

where R is the universal gas constant [$8.314\,\mathrm{J\,(mol{\cdot}K)^{-1}}$] and T is the temperature in Kelvin.

A plug-flow reactor assumes gas goes through the reactor as a 'plug' and there is no axial diffusion. The plug-flow reactor design equation,

$$V = v[\mathrm{NH_3}] \int_0^X \frac{\mathrm{d}X}{-\mathrm{d}[\mathrm{NH_3}]/\mathrm{d}t}, \tag{3}$$

can be solved for conversion, X:

$$X = 1 - \exp\left[k_0 \exp\left(-\frac{E}{RT}\right)\tau\right] \tag{4}$$

where V is the volume of the reactor, v is the volumetric flowrate, and τ is the residence time. As the residence time for the reaction is small, the reaction conversion does not change much if the reactor were modeled as a continuously stirred tank reactor.

The model assumes that the reaction occurs only in the MHC cylindrical hole and decomposition results from solely thermal processes. The residence time is calculated for the gas velocity going through a reactor 500 μm long. In addition to affecting the rate constant of the reaction, the temperature also affects the density of the gas. To conserve mass flow,

the velocity of the gas in the reactor will change. With a change in gas velocity, the residence time of the reaction changes. The reaction temperature then must be calculated to satisfy both the reaction kinetics and the residence times used to calculate the reaction kinetics. The calculations are iterated until a self-consistent reaction temperature is obtained. The model does not take into account the change in moles of gas with reaction.

For the data at an upstream pressure of 100 Torr and power of 4.3 W in Fig. 5, the calculated reaction temperature is 2960 K. For the same pressure but a power of 5.8 W, the calculated temperature is 3080 K. The 33% increase in power increased the reaction temperature by only 4%.

These calculated temperatures are higher than the reported temperatures of 1000–2000 K. For purely thermal ammonia decomposition occurring at 2000 K and the residence times tested, less than 0.01% of the ammonia would be converted. There are a few possible reasons for this discrepancy. Reactive plasma species, such as ions and radicals, may enhance the reaction to boost the effective reaction temperature. In addition, the reaction is not limited to the MHC hole. OES temperature measurements were conducted in nitrogen, not ammonia.

An increase in the pressure from 100 to 700 Torr increases conversion (Fig. 6). This is expected because at a higher pressure, a lower gas velocity is needed to deliver the same standard flowrate. With a lower gas velocity, the residence time is higher. Even though the conversion increased for a higher pressure, the data are close to the same temperature as the lower

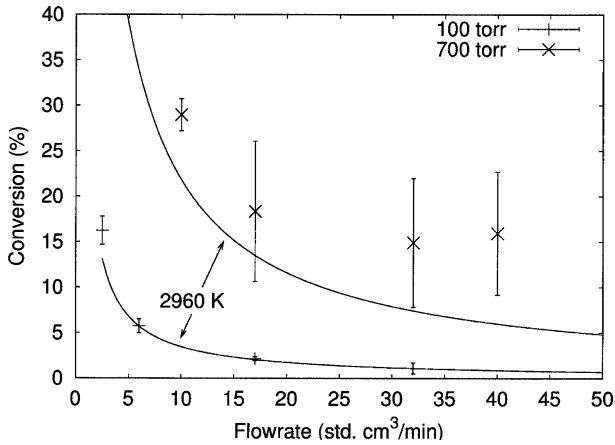

Fig. 6. NH_3 conversion as a function of flowrate and pressure. An increase in pressure increases the conversion by increasing the residence time for the same standard flowrate. The 100 Torr data points are the same as 4.3 W points in Fig. 5.

pressure data, as the residence time for the 700 Torr case is seven times longer than the 100 Torr case. If the data are plotted against residence time instead of flowrate as in Fig. 7, the data are near the conversion predicted by the thermal decomposition model. Larger error was present with 700 Torr runs at higher flowrates. This may have been a result of larger pressure increases in the system with the plasma on. While part of the increased conversion may be a result of increased current densities at higher pressures,[12] the ammonia conversion did not increase proportionally to the square of the pressure. Thus, the effect of residence time is likely the most significant factor.

3.2. Carbon Dioxide

The cracking of carbon dioxide by MHC is measured by both mass spectrometer and FTIR. Figure 8 shows the results of one run in the mass spectrometer. Similar results were seen in the FTIR. Although carbon monoxide could decompose to form carbon and oxygen, the further decomposition of carbon monoxide does not exceed 35% even under reaction temperatures as high as 7500 K.[13] In our analysis, decomposition of carbon monoxide is neglected. The steady state levels of carbon dioxide while the plasma was on and off are used to calculate conversion.

As in the ammonia experiments, the effect of flowrate on conversion is studied. As the flowrate increases, the conversion of carbon dioxide decreases (Fig. 9). An increase in up-stream pressure from 150 to 250 Torr increases conversion. The upstream pressure of 250 Torr is the maximum

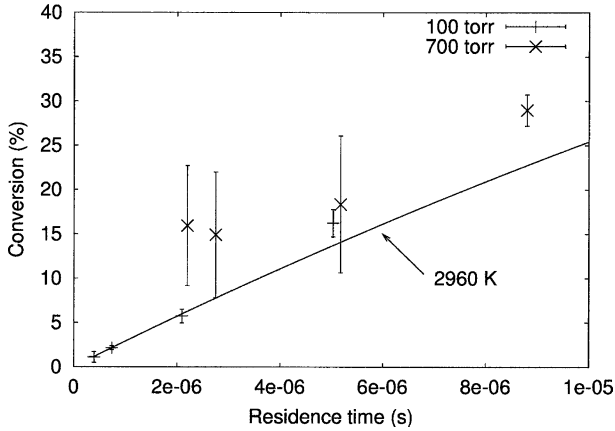

Fig. 7. NH_3 conversion as a function of residence time for the same data shown in Fig. 6.

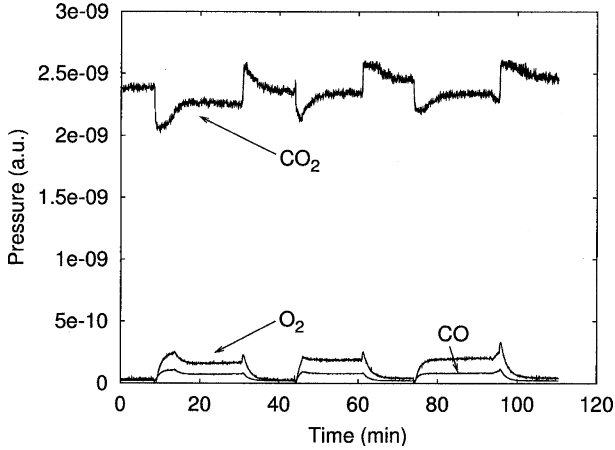

Fig. 8. Mass spectrometer signals of carbon dioxide decomposition for 19 sccm, 150 Torr upstream pressure and 5.2 W. When the plasma is on, carbon dioxide decreases, while carbon monoxide and oxygen increase.

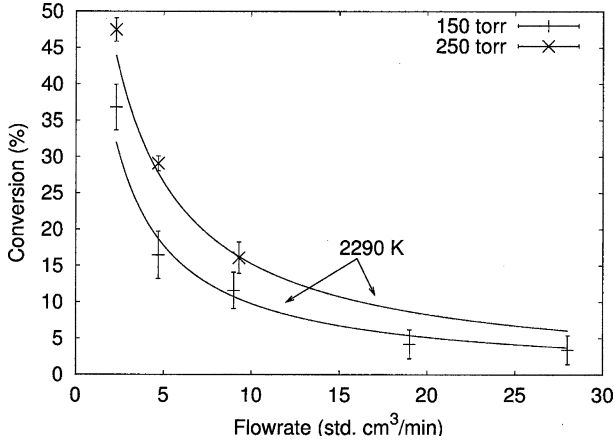

Fig. 9. CO_2 conversion as a function of flowrate for two operating pressures. Both sets of data are fit to the same effective reaction temperature.

pressure which would allow steady-state operation. The data are fit to a plug-flow reactor model and the kinetic data.[14] The kinetic dissociation rate, k_d, for the reaction is

$$k_d = 7.5 \times 10^{12} T^{\frac{1}{2}} \exp\left(-\frac{1.04 \times 10^5}{RT}\right) \frac{\text{cm}^3}{\text{mol} \cdot \text{s}}. \tag{5}$$

The reaction temperature is calculated for carbon dioxide decomposition in the same manner that the temperature is calculated for ammonia decomposition. Both the data from the 150 and 250 Torr experiments correspond to a reaction temperature of 2290 K. As in the ammonia experiments, we see a high reaction temperature.

3.3. MHCDs in Series

The results of runs when operating two plasmas in series are shown in Fig. 10 and Table II. The conversion with both plasmas on is the summation of the individual conversions of each plasma. Although no enhancement of the reaction occurs, the results suggest that when several of these plasmas are put in series, the conversion would be equivalent to a reactor volume equal to the summation of the individual plasma volumes. Subsequent plasmas also operate at lower pressure and could thus operate at lower powers. This is consistent with a plug-flow reactor model.

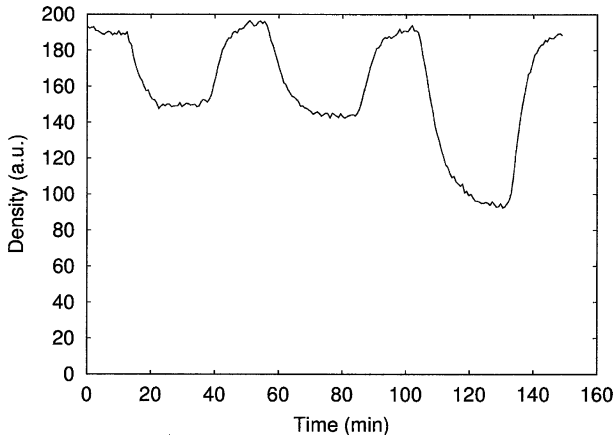

Fig. 10. Fourier transform infrared (FTIR) results of NH_3 decomposition with plasmas in series at 4.7 W, 110 Torr upstream pressure. The first decrease in signal is a result of only the upstream plasma. The second decrease is a result of only the downstream plasma. The third decrease is a result of both plasmas on.

Table II. Conversion of Ammonia in Microhollow Cathode's Discharges in Series

	Upstream	Downstream	Both
Conversion (%)	6.8 ± 2.2	8.9 ± 1.0	16.3 ± 3.0

3.4. Pressure and MHC-Lumped Conductance Model

In order to confirm the interpretation of the FTIR and mass spectrometer data, a model of the flows and conductances of the apparatus is used. The model could be used to determine whether the surges and dips in mass spectrometer data in Fig. 8 are a result of the temperature changes in the MHC or actual changes in gas density. Most importantly, the model would confirm that the difference in the reading with the plasma off and the reading with the plasma on is indeed the percent conversion, rather than an artifact of changes in pressure or factors not related to gas density.

Additionally, the plasma affects the pressure in the system and such effects would have process design implications. When the plasma is on, the pressure upstream of the plasma rises to a new steady state, and the pressure downstream of the plasma will decrease initially. When the plasma is turned on, the temperature in the region rises. An increase in temperature decreases gas density. In order to maintain the same mass flowrate, the pressure drop must increase. Such phenomena have been explained and modeled using finite element analysis.[15] The lumped conductance model would verify whether the pressure changes seen in the system are the result of a decrease in conductance after turning on the plasma.

The geometry used to model the experimental apparatus (Fig. 2) is shown in Fig. 11. This consists of two volumes, of sizes V_0 and V_1 and at pressures of P_0 and P_1, respectively. These volumes are connected by the MHC orifice, modeled as a volumeless section with a conductance of C_1. A flowrate of Q_0 is fed to V_0. The system is pumped out by a pump at constant pressure, P_p, connected to V_1, by a valve of conductance, C_v. The volumes are isothermal; a rise in the temperature of the MHC orifice is assumed not to have an effect on the temperatures of the surrounding volumes. This system can be described by the ordinary differential equations shown in Eqs. (6) and (7):

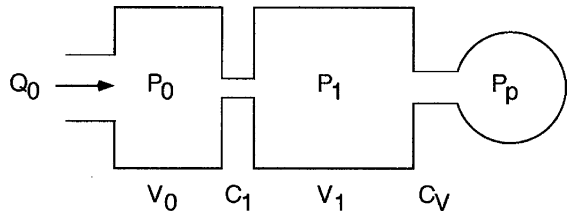

Fig. 11. Two-volume geometry used in lumped conductance model.

$$Q_0 - C_1(P_0 - P_1) = V_0 \frac{dP_0}{dt} \tag{6}$$

$$C_1(P_0 - P_1) - C_v(P_1 - P_p) = V_1 \frac{dP_1}{dt} \tag{7}$$

We can determine experimentally the conductances of the orifice and valve, given the flowrate and the pressure drops at steady state. Flowrates of 0.201 and 0.401 Torr-L/s (15.8 and 31.7 sccm, respectively) of nitrogen were used. The upstream pressure, P_0, was measured by a convection gauge, and the dowstream pressure, P_1, was measured by a capacitance manometer gauge. The resulting pressures are shown in Fig. 12. The pressure changes for the convection gauge were not as smooth as for the capacitance manometer. The convection gauge, at pressures around 200 Torr, was only accurate to ± 5 Torr. The pump pressure, P_p, is 60 m Torr.

The volumes and conductances of each section are solved using Eqs. (6) and (7). The slopes of the pressure curves at various times are used for the derivative terms to calculate the volume. These volumes are averaged. The resulting conductances and volumes are listed in Table III.

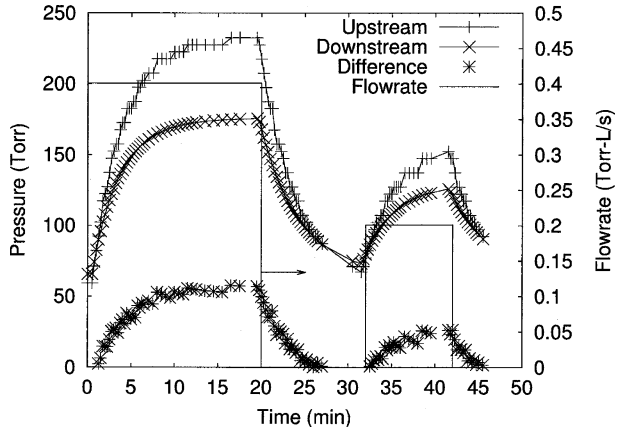

Fig. 12. Pressure changes with a flowrate of 0.401 Torr L/s from 0 to 20 min and a flowrate of 0.201 Torr L/s from 32 to 42 min.

Table III. Experimental Values of Conductance Model Parameters

Parameter (unit)	Average
C_1(L/s)	0.00739
C_v(L/s)	0.00192
V_0(L)	0.00789
V_1(L)	0.014

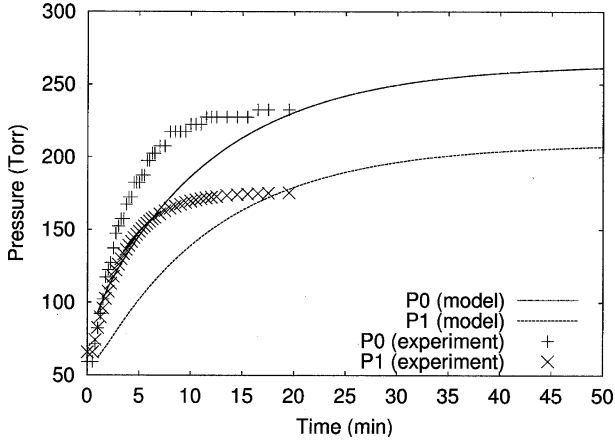

Fig. 13. Experimental and simulated pressure increases for both volumes with a flowrate of 0.401 Torr L/s.

The pressure increases are simulated by solving the system of two ordinary differential equations, Eqs. (6) and (7). The simulated pressure increases are shown in Figs. 13 and 14. For the lower flowrate, the simulation underestimates the steady-state pressures by approximately 30 Torr for both volumes. For the higher flowrate, the simulation overestimates the steady-state pressures by approximately 30 Torr for both volumes. The shapes of the pressure curve are similar as those found in experiment. The

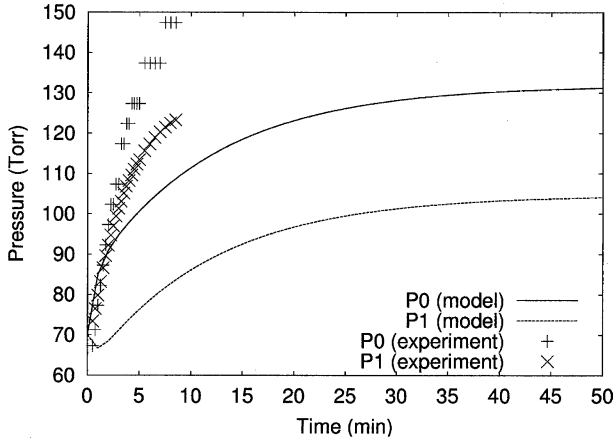

Fig. 14. Experimental and simulated pressure increases for both volumes with a flowrate of 0.201 Torr L/s.

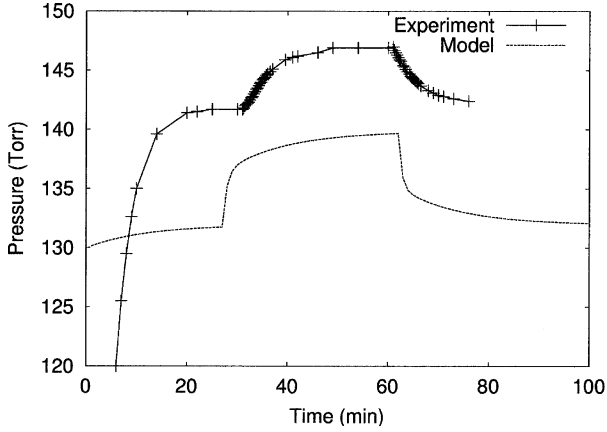

Fig. 15. Experiment and model comparison of P_0, turning on a plasma at 31 min (model turns on at 27 min) and turning off the plasma at 62 min.

times to reach 95% of the steady-state pressures are approximately 21 min longer than those found in the experiment.

The change in the conductance of the orifice, C_1, when a plasma is turned on is also tested. In an experiment, a plasma in a flow of 0.201 Torr-L/s of nitrogen is turned on, and the pressures in both volumes is monitored. The pressures are measured with a capacitance manometer in two separate experiments. These results are represented as points in Figs. 15 and 16.

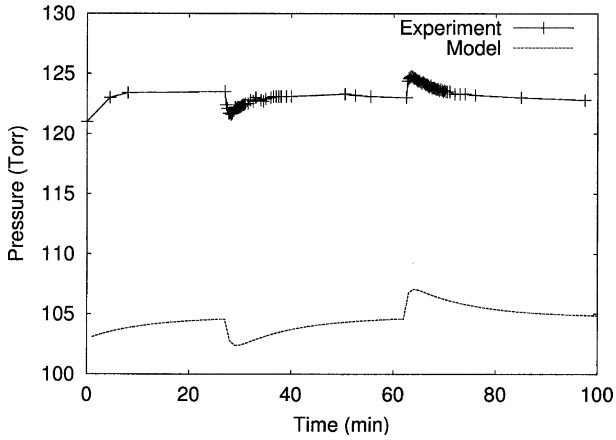

Fig. 16. Experimental and model comparison of P_1, turning on the plasma at 27 min and off at 62 min.

When the plasma is turned on, the upstream pressure increases as a result of the decreased conductance of the orifice. This can be seen in Eq. (6). The system is initially at a steady-state pressure. When the conductance, C_1, decreases, dP_0/dt becomes positive. However, the downstream pressure, P_1, drops initially when the plasma is turned on. As shown in Eq. (7), when C_1, drops, dP_1/dt must be negative. As the upstream pressure increases, the $C_1(P_0 - P_1)$ term eventually equals Q_0. With those terms equal, Eq. (7) will be the same as when the system was at steady state and the plasma was off. P_1 must then return to the same pressure as when the plasma was off.

In our model, the plasma is turned on at 27 min (to coincide with the run measuring P_1) thereby decreasing the conductance of the orifice. In this case, the conductance decreases by a factor of 1.29, from 0.00192 to 0.00149 L/s. This conductance is chosen to match the magnitudes of the pressure changes found experimentally. The plasma is turned off at 62 min, increasing the conductance back to the original value. The model results are shown in Figs. 15 and 16. The simulated shapes of the pressure curves are similar to those found in experiments. As noted earlier, the calculated times to reach the initial steady state when flowing in the gas with no plasma on is longer than in experiment. However, once this steady state is reached, the response of the pressures in the model to a change in conductance is similar to what is found in experiment. As both the mass spectrometer and FTIR sample from gas downstream of the plasma, Fig. 16 shows that any change in the steady-state readings of the FTIR and the mass spectrometer are the result of concentration changes and not pressure changes.

This simple lumped conductance model verifies that changes in pressure seen experimentally are a result of a change in conductance of the MHC orifice. The cause of the change in conductance is presumably the result of temperature changes because of the plasma.

4. CONCLUSIONS

The experiments presented in this paper showed significant decomposition of NH_3 and CO_2, occurring with effective reaction temperatures exceeding 2000 K. Based on these results, thermal processes play an important role in the reaction chemistry in the MHCD. A simple model based only on thermal decomposition can be used to effectively predict the conversion response as a result of the changes in flow rate and pressure. However, because the effective reaction temperatures are higher than the reported temperatures for MHCD's, it seems likely that part of the decomposition kinetics are because of the reactive plasma ions and

electrons, in addition to purely thermal processes. Experiments with more than one MHC in series increase conversion significantly. Pressure changes are observed in the volumes upstream and downstream of the plasma when the plasma was toggled on or off. Such behavior is modeled with a lumped conductance model, which relates the pressure behavior to a decrease in conductance with the plasma on, which would be consistent with the MHCD increasing the temperature in the discharge hole. The conversions seen in the MHCD in these experiments are lower than what could be achieved in a lower temperature, but larger, microreactors. However, the MHCD has a high reaction temperature occurs in a naturally small space, without the need to scale down, unlike with resistive heaters. This key advantage could be exploited as '-on-a-chip' systems become smaller and smaller.

ACKNOWLEDGMENTS

The authors thank Heywood Kan and Chad Su for experimental assistance. This work is supported in part by Kodak and a National Science Foundation fellowship.

REFERENCES

1. M. Freemantle, *Chem. Eng. News* **77**, 27 (1999).
2. R. Srinivasan et al., *Am. Inst. Chem. Eng. J.* **43**, 3059 (1997).
3. F. Leipold, R. H. Stark, A. El-Habachi, and K. H. Schoenbach, *J. Phys. D: Appl. Phys.* **33**, 2268 (2000).
4. C. Penache et al., *Plasma Sources Sci. Technol.* **11**, 476 (2002).
5. S. L. Firebaugh and M. A. Schmidt, *J. Microelectromech. Syst.* **7**, 128 (1998).
6. T. Sakurai and A. Yokoyama, *J. Nucl. Sci. Tech.* **37**, 814 (2000).
7. K. H. Schoenbach, R. Verhappen, T. Tessnow, and F. E. Peterkin, *Appl. Phys. Lett.* **68**, 13 (1996).
8. K. H. Schoenbach, A. El-Habachi, W. Shi, and M. Ciocca, *Plasma Sources Sci. Technol.* **6**, 468 (1997).
9. A. D. White, *J. Appl. Phys.* **30**, 711 (1959).
10. D. F. Davidson, K. Kohse-Höinghaus, A. Y. Chang, and R. K. Hanson, *Intl. J. Chem. Kinet.* **22**, 513 (1990).
11. A. A. Konnov and J. DeRuyck, *Combust. Sci. Tech.* **152**, 23 (2000).
12. M. Moselhy, W. Shi, R. H. Stark, and K. H. Schoenbach, *IEEE Trans. Plasma Sci.* **30**, 198 (2002).
13. Y. Nishimura, T. Takenouchi, and W. Sakai, *Bull. Chem. Soc. Jap.* **47**, 2331 (1974).
14. N. A. Ebrahim and R. J. Sandeman, *J. Chem. Phys.* **65**, 3446 (1976).
15. M. A. Nierode, Neutral Gas Pressure Profiles in Flowing, Non-equilibrium Plasmas, Master's Thesis, University of California, Berkeley, CA, 2003.